

# Linear Dichroism Measurements on Oriented Purple Membranes between Parallel Polarizers: Contribution of Linear Birefringence and Applications to Chromophore Isomerization

Berthold Borucki, Harald Otto, and Maarten P. Heyn\*

Biophysics Group, Physics Department, Freie Universität Berlin, Arnimallee 14, D-14195 Berlin, Germany

Received: December 9, 1997; In Final Form: February 18, 1998

Absorption measurements with linearly polarized light were performed with oriented purple membranes in the wavelength range from 350 to 750 nm. The membranes were oriented in a magnetic field and subsequently immobilized in a gel. Alternatively orientation was achieved by anisotropic swelling of a dehydrated gel. This new method of orientation, which is similar to the gel-squeezing technique, yields a negative second-order parameter  $S_2$  (e.g., the membranes orient preferentially with their planes parallel to the direction of expansion). In contrast to standard linear dichroism measurements, we used a setup where the oriented sample is inbetween two parallel polarizers. The dependence of the transmitted intensity on the angle between the orientation axis and the polarizer direction shows that the phase difference due to linear birefringence contributes substantially to the signal. Experimental data of high accuracy were obtained by taking measurements at 14 angles from  $-20^\circ$  to  $110^\circ$  in steps of  $10^\circ$ . Fitting of the polarization data at each wavelength yields the absorption spectrum, the anisotropy and the linear birefringence. Analogous measurements were carried out on chromophore-free samples to correct for light scattering and to extract the chromophore contribution to the linear birefringence. The chromophore part of the linear birefringence is in good agreement with numerical calculations from absorption and anisotropy via the Kramers–Kronig transform. The method was applied to investigate possible changes in transition dipole moment orientation associated with the isomerization of the chromophore in light–dark adaptation (all-trans to 13-cis) and the blue–pink transition (all-trans to 9-cis). Analysis of the anisotropy indicates that there is no change in the orientation of the transition dipole moment with respect to the orientation axis between the light and dark adapted states. Only a small increase ( $\approx 2.5^\circ$ ) of the chromophore angle occurs between the blue state and the pink state. Comparison of the measured birefringence changes and the calculations from absorption and anisotropy changes confirm the validity of the approach.

## 1. Introduction

Polarized absorption spectroscopy is a useful method to obtain structural information on the orientation of chromophores. In the case of purple membranes from *Halobacterium salinarum*, it has been used to determine the orientation of the retinal transition dipole moment with respect to the membrane normal by steady-state spectroscopy on thin purple membrane films.<sup>1,2</sup> In order to study various chromophore states, which may differ in the orientation of the transition dipole moment, it is advantageous to orient and immobilize purple membranes in a gel. In contrast to thin and partially dehydrated films, orientation and immobilization in polyacrylamide gels permit well-defined conditions of pH and ionic strength in an aqueous environment. The photochemical, functional and spectral properties of purple membranes are not affected by the gel.<sup>3</sup> Moreover, the beam geometry in experiments with oriented gel samples is simpler (e.g., the probe beam is perpendicular to the orientation axis of the sample, and thus less susceptible to experimental artifacts).

In the photocycle of bacteriorhodopsin the chromophore passes thru a sequence of transient optical states, which may be monitored by time-resolved polarized absorption spectroscopy.

copy.<sup>4,5</sup> It has been shown previously<sup>6</sup> that isotropic excitation of oriented samples provides the most accurate information on the orientation of the transition dipole moment in transient states. However, in practice, this method is limited to chromophore states which occur in completely reversible cycles with maximum decay times of about 10 s. For chromophore states which are formed by very slow thermal relaxation (i.e., 13-cis-15-syn retinal in light–dark adaptation<sup>7</sup>), by changing of external parameters (i.e., formation of the blue state by decreasing pH<sup>8</sup>) or by photoconversion with very low quantum efficiency (i.e., formation of the pink 9-cis state by illumination of the blue state with red light<sup>9,10</sup>), it is advisable to go back to steady-state measurements.

The linear dichroism of the oriented sample is usually determined by measurements of the absorption with polarizers parallel ( $A_{||}$ ) and perpendicular ( $A_{\perp}$ ) to the orientation axis of the sample. Higher accuracy is achieved by measurements of the absorption as a function of the polarization angle (e.g., variation of the polarization angle in steps of  $10^\circ$ ). This has already been demonstrated by Schertler et al.,<sup>11</sup> who used crystals of bacteriorhodopsin. In the crystals the bR molecules are not in their native environment however. The analysis they used requires that the efficiency of the detection system doesn't depend on the state of polarization of the light emerging from the sample. However, this is not generally fulfilled.

\* To whom correspondence should be addressed. Fax: 49-30-838-5186. E-mail: HEYN@PHYSIK.FU-BERLIN.DE.

To avoid these experimental problems, we introduced a second polarizer, which is placed in the measuring beam behind the oriented sample and is adjusted parallel to the first polarizer. The transmitted intensity of this setup depends not only on the linear dichroism, but is also affected by linear birefringence. In this paper we will present the equations which describe the dependence of the transmitted intensity on the polarization angle in this geometry. A three parameter fit yields the (isotropic) absorption, the corresponding anisotropy, and the phase difference due to linear birefringence at each wavelength. An additional parameter, which should be in principle identical for all wavelengths, takes into account that the zero point of the polarizer angles might not be adjusted perfectly to the orientation axis of the sample. The linear birefringence of oriented purple membranes in a homogeneous medium like a polyacrylamide gel is composed of form birefringence and intrinsic birefringence. The form birefringence arises from the ordered arrangement of particles of nonspherical shape, such as the membranes, in a medium of different refractive index. The material of the membranes may be optically isotropic. In contrast, the intrinsic birefringence reflects the anisotropic optical properties of the material of the membranes. Mathematical expressions, considering axially symmetric particles in dilute solutions, were already derived by Peterlin and Stuart.<sup>12</sup> In the case of purple membranes, the absorbing molecules contribute to the intrinsic birefringence, since absorption and dispersion are connected by the Kramers–Kronig transform. Zeisel and Hampp<sup>13</sup> provided experimental evidence that absorption contributes to the refractive index, but only the spectral relationship of refractive index and absorption changes was demonstrated and normalization of their data was required. The nonchromophoric contributions to the birefringence of the oriented purple membrane sample may be determined by measurements on the bleached (e.g., chromophore free) sample. We will show that all contributions to the linear birefringence are of the same order of magnitude, and that the chromophore part is in good agreement with the calculations from absorption and anisotropy via the Kramers–Kronig transform. The experimental method and the analysis was applied to changes in the isomerization state of the chromophore of bacteriorhodopsin (i.e., light–dark adaptation and the blue–pink transition). Information on the chromophore part of the linear birefringence and comparison with the calculations from absorption and anisotropy serve as a valuable criterion for the correct determination of the linear dichroism (e.g., the anisotropy).

The orientation of purple membranes in high magnetic fields is a well-established method.<sup>3,6,14,15</sup> The purple membranes orient with their normals parallel to the field direction. If the membranes are perfectly planar, a high degree of orientation is reached (second order parameter  $S_2 = 1$  in maximum, for definition of  $S_2$  see eq 10). But if the membranes are curved or rolled, and this might be the case in the absence of salt and buffer, the orientation in magnetic fields is poor. To avoid these difficulties, we developed an alternative method of orienting purple membranes, which is analogous to the compression of gels in two directions.<sup>16</sup> Isotropic drying and anisotropic swelling of polyacrylamide gels produces nearly perfectly oriented samples, with the membrane planes orienting preferentially parallel to the direction of expansion. In this case the order parameter  $S_2$  reaches maximal values of  $-0.5$ . Though the maximal degree of orientation is not as favorable as in magnetically oriented samples, we get closer to the optimum and obtain an even higher absolute value for the order parameter  $S_2$  than we do for the case of magnetically ordered purple

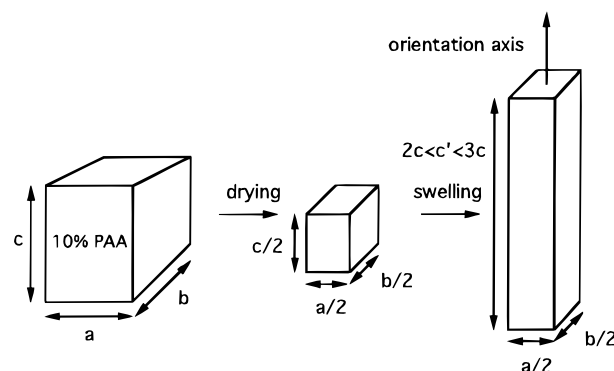


**Figure 1.** Schematic representation of the orientation by drying and anisotropic swelling. First step: the isotropic gel (water content  $\approx 90\%$ ) with dimensions  $a$ ,  $b$ ,  $c$  dries and shrinks to the final dimensions less than  $a/2$ ,  $b/2$ ,  $c/2$  (water content  $\approx 0\%$ ). Second step: the gel is induced to swell in a cuvette of cross-section  $a/2 \times b/2$ ; expansion is allowed only in the  $z$ -direction. The final volume is smaller than the initial volume before the drying process.

membranes, especially in preparations without salt and buffer. Stress birefringence due to the expanded nonisotropic polyacrylamide gel has to be taken into account and may dominate the other contributions in certain wavelength regions.

## 2. Materials and Methods

**2.1. Preparation of Oriented PM Samples.** The orientation of the purple membranes was achieved by two different methods: (1) orientation in a high magnetic field and immobilization in a gel, (2) alignment by swelling of dehydrated isotropic polyacrylamide gels.

(1) The orientation of purple membranes in high magnetic fields and immobilization in polyacrylamide gels is a well-established method.<sup>3,6,14</sup> We used suspensions containing 15  $\mu\text{M}$  bR (bacteriorhodopsin), 15 mM Tris buffer (pH 7), 75 mM KCl, and 10% acrylamide. The polymerization was started by adding APS (ammonium persulfate, 1.37 mM) and TEMED ( $N,N,N',N'$ -tetramethylethyldiamine, 1.65 mM). The suspensions were filled in standard  $4 \times 10$  mm quartz cuvettes, which were placed in a 14 T superconducting magnet. The patch planes orient preferentially perpendicular to the direction of the magnetic field [e.g., the second-order parameter  $S_2 = \langle P_2(\cos \vartheta) \rangle$  (where  $\vartheta$  is the angle of the membrane normal with respect to the direction of the magnetic field) is positive and reaches 1.0 for perfect orientation].

(2) The orientation by swelling is in principle similar to the gel-squeezing technique,<sup>16,17</sup> but it is much easier and doesn't require a complicated mechanical setup. We started with an isotropic 10% PAA (polyacrylamide) gel containing purple membranes, which was prepared in a cuvette of  $10 \times 10$  mm cross section (see Figure 1). Because the water content of the gel is nearly 90%, the volume shrinks to 10% of the initial volume when the gel is completely dried. This dried gel was placed in another cuvette of only  $5 \times 5$  mm cross section and was induced to swell by adding (deionized) water. Expansion is only possible in one direction due to the dimensions of the cuvette. During the swelling process, the purple membranes orient preferentially parallel to the direction of expansion (e.g.,  $S_2$  is negative and reaches  $-0.5$  in the case of perfect orientation). The swelling procedure takes about 4–8 weeks and a final volume is reached, which is about 20–30% smaller than the initial volume before the drying process. To convert the purple membranes to the blue state, we used 15 mM acetic acid (pH 2.5) instead of pure (deionized) water in the swelling procedure.

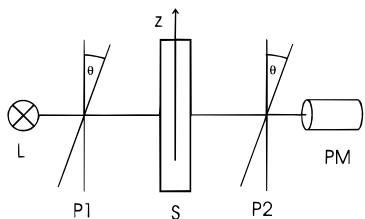


**Figure 2.** Geometry of the polarization setup. The sample *S*, with orientation axis in *z*-direction, is placed between two parallel polarizers *P1* and *P2*. Both polarizers make an angle of  $\theta$  with the *z*-axis.

**2.2. Polarized Steady-State Measurements.** The polarized spectra were measured in a Shimadzu UV-2102PC spectrophotometer in the absorption mode. The oriented sample was placed between two Glan–Taylor polarizers, which are parallel and have to be moved simultaneously (Figure 2). For higher accuracy, we measured at 14 polarization angles (e.g., from  $-20^\circ$  to  $110^\circ$  in steps of  $10^\circ$ ), although in principle the full information is contained in the measurement of only three polarization angles, assuming that the orientation axis of the sample coincides with the  $0^\circ$ -position of the polarizers. The magnetically oriented sample was measured in the light-adapted state and dark-adapted state (relaxation about 24 h in the dark at room temperature). An oriented bleached sample provided an appropriate reference for the light scattering and birefringence background. Averaging of all measured spectra over 5 nm intervals produced reduced spectra.

**2.3. Bleaching of the Samples.** The bleaching was carried out with a 1000 W xenon arc lamp and a cut-off filter WG305. Control spectra showed that only the chromophore is destroyed and the aromatic amino acids are unaffected. The two photoproducts,<sup>18</sup> which appeared already after a short time of illumination, also completely degraded with further irradiation. Heating damage to the membranes or the protein structure was prevented by keeping the temperature below  $40^\circ\text{C}$ . The irradiation took about 90 min.

**2.4. Blue–Pink Transition.** Samples, which were oriented by swelling in 15 mM acetic acid (pH 2.5) during 6 weeks in the dark, were used to measure the optical properties of the membranes with bR in the dark-adapted blue state. Illumination with red light (fiber lamp, 150 W tungsten halogen, cut-off filter RG610) induces transitions to the pink state.<sup>9,10</sup> Spatially uniform illumination of about 9 min duration reduced the population of the blue state to 20% of the initial concentration. Since the blue to pink transition is partially irreversible and since the pink-state is thermally not stable (decay time at room temperature  $\approx 300$  min), we modified our measuring scheme: the number of polarization angles was reduced to only four ( $0^\circ$ ,  $90^\circ$ ,  $30^\circ$ , and  $60^\circ$ ), but this sequence was repeated five times. For each polarization angle, the spectra were extrapolated to the initial state (e.g., the time, when the first spectrum was measured). We also bleached this sample as a reference for light scattering and birefringence background and carried out the polarized measurements in the original scheme (14 polarization angles).

**3. Data Analysis and Basic Calculations.** To analyze our data it is convenient to use the Jones calculus.<sup>19,20</sup> We start with the Jones vector, which represents the electric field vector emerging from the first polarizer, which makes an angle  $\theta$  with the orientation axis (Figure 2):

$$\vec{\epsilon} = \begin{pmatrix} \epsilon_{\parallel} \\ \epsilon_{\perp} \end{pmatrix} = \epsilon_0 \begin{pmatrix} \cos \theta \\ \sin \theta \end{pmatrix} \quad (1)$$

The anisotropically absorbing, scattering and phase changing sample with optical axis parallel to  $(1,0)^T$  is represented by the Jones matrix:

$$\mathbf{M}_1 = \begin{pmatrix} 10^{-E_{\parallel}/2} e^{i\phi_{\parallel}} & 0 \\ 0 & 10^{-E_{\perp}/2} e^{i\phi_{\perp}} \end{pmatrix} \quad (2)$$

where  $E_{\parallel} = A_{\parallel} + S_{\parallel}$  and  $E_{\perp} = A_{\perp} + S_{\perp}$  are defined as the extinctions for radiation polarized parallel and perpendicular to the optical axis;  $\phi_{\parallel}$  and  $\phi_{\perp}$  are the corresponding phase changes (parallel and perpendicular). Absorption *A* and light scattering *S* are considered to be independent processes and to obey Lambert–Beer’s law. The Jones matrix for a polarizer at angle  $\theta$  with respect to the optical axis of the sample is given by

$$\mathbf{M}_2 = \begin{pmatrix} \cos^2 \theta & \sin \theta \cos \theta \\ \sin \theta \cos \theta & \sin^2 \theta \end{pmatrix} \quad (3)$$

The electric field vector emerging from the second polarizer is thus

$$\begin{aligned} \vec{\epsilon}' &= \mathbf{M}_2 \mathbf{M}_1 \vec{\epsilon} \\ &= \epsilon_0 (\cos^2 \theta 10^{-E_{\parallel}/2} e^{i\phi_{\parallel}} + \sin^2 \theta 10^{-E_{\perp}/2} e^{i\phi_{\perp}}) \begin{pmatrix} \cos \theta \\ \sin \theta \end{pmatrix} \end{aligned} \quad (4)$$

This leads to the following expression for the intensity, which is transmitted by a setup of two parallel polarizers and an oriented sample inbetween

$$\begin{aligned} I(\theta) &= \vec{\epsilon}'(\vec{\epsilon}')^* \\ &= \epsilon_0^2 [\cos^4 \theta 10^{-E_{\parallel}} + \sin^4 \theta 10^{-E_{\perp}} + \\ &\quad 2 \cos^2 \theta \sin^2 \theta 10^{-E_{\parallel}/2 - E_{\perp}/2} \cos(\phi_{\parallel} - \phi_{\perp})] \end{aligned} \quad (5)$$

Introducing the isotropic extinction  $E_0 = (E_{\parallel} + 2E_{\perp})/3$ , the related anisotropy  $r_E = (E_{\parallel} - E_{\perp})/(E_{\parallel} + 2E_{\perp})$ , as well as the phase difference  $\Delta\phi_E = \phi_{\parallel} - \phi_{\perp}$ , we define the extinction at polarization angle  $\theta$ :

$$\begin{aligned} E(\lambda, \theta) &= \log \frac{I(\lambda, \theta, E_0 = 0, r_E = 0, \Delta\phi_E = 0)}{I(\lambda, \theta, E_0, r_E, \Delta\phi_E)} \\ &= E_0(1 - r_E) - \log[\cos^4 \theta 10^{-3E_0 r_E} + \sin^4 \theta + \\ &\quad 2 \cos^2 \theta \sin^2 \theta 10^{-3/2 E_0 r_E} \cos(\Delta\phi_E)] \end{aligned} \quad (6)$$

$E(\lambda, \theta)$  depends on the three wavelength-dependent parameters  $E_0$ ,  $r_E$ , and  $\Delta\phi_E$ . The value of  $\Delta\phi_E$  is not unique, since  $\cos(\Delta\phi_E) = \cos(\pm\Delta\phi_E + 2\pi m)$  with  $m$  an integer. We note that it follows from the third term in the argument of the logarithm of eq 6 that linear birefringence contributes at all angles except when either  $\cos \theta$  or  $\sin \theta$  is zero.

Decomposing extinction in absorption and scattering, we get from  $E_0$ ,  $r_E$ , and  $\Delta\phi_E$ :

$$\begin{aligned} E_0 &= A_0 + S_0, \quad E_0 r_E = A_0 r_A + S_0 r_S, \quad \text{and} \\ \Delta\phi_E &= \Delta\phi_A + \Delta\phi_S \end{aligned} \quad (7)$$

where  $A_0$  is the isotropic absorption,  $r_A$  the absorption anisotropy,  $S_0$  the isotropic scattering,  $r_S$  the scattering anisotropy,

$\Delta\phi_A$  the phase difference due to the chromophore absorption, and  $\Delta\phi_S$  the phase difference due to form birefringence and intrinsic birefringence of chromophore-free membranes.

Measurements on the chromophore free membrane sample ( $A_0 \equiv 0$  and  $\Delta\phi_A \equiv 0$ ) allow us to determine  $S_0$ ,  $r_S$ , and  $\Delta\phi_S$ . From these parameters we get with eq 7  $A_0$ ,  $r_A$ , and  $\Delta\phi_A$ , which are the physically interesting quantities.

The phase difference  $\Delta\phi$  and the linear birefringence  $\Delta n = n_{||} - n_{\perp}$  (e.g., anisotropy of the refractive index) obey the following relation (with  $d$  = light path through the sample,  $\lambda$  = wavelength):

$$\Delta n_E = \frac{\Delta\phi_E \lambda}{2\pi d} = \frac{(\Delta\phi_A + \Delta\phi_S) \lambda}{2\pi d} = \Delta n_A + \Delta n_S \quad (8)$$

In analogy to the phase differences,  $\Delta n_A$  is the contribution of the chromophore (anomalous dispersion) (i.e., only intrinsic birefringence), while  $\Delta n_S$  may include intrinsic and form birefringence.

The phenomenon of linear birefringence in dilute solutions has already been analyzed by Peterlin and Stuart.<sup>12</sup> Assuming axially symmetric particles, they derived

$$\Delta n = \frac{2\pi C_V}{n} (g_1 - g_2) S_2 \quad (9)$$

where  $\Delta n = n_{||} - n_{\perp}$ ,  $n$  is the refractive index of the solution,  $C_V$  is the volume fraction of particles, and  $(g_1 - g_2)$  is the optical anisotropy factor. The subscripts 1 and 2 refer to the symmetry and transverse axes, respectively.  $S_2$ , the second-order parameter, is defined as

$$S_2 = \langle P_2(\cos \vartheta) \rangle \quad (10)$$

where  $\vartheta$  is the angle of the membrane normal with respect to the direction of the magnetic field and the average is over the orientational distribution of the membrane normals. In the case of disc-shaped particles (ellipsoid with symmetry axis  $a_1 \rightarrow 0$ , an appropriate approximation for the flat purple membranes), the original expression of Peterlin and Stuart reduces to

$$g_1 - g_2 = \frac{n_l^2}{4\pi n_1^2} (n_1^2 - n_2^2) - \frac{1}{4\pi n_1^2} (n_1^2 - n_l^2) (n_2^2 - n_l^2) \quad (11)$$

where  $n_l$  is the refractive index of the solvent;  $n_1$ ,  $n_2$  are the refractive indices of the particle in the direction of the symmetry and transverse axis, respectively. The first part in eq 11 is due to the intrinsic anisotropy, while the second part is due to the form anisotropy.

Introducing the average refractive index of the particles  $\bar{n} = (n_1 + n_2)/2$ , and using the approximation  $n_1^2 \approx \bar{n}^2$ ,  $n_2^2 \approx \bar{n}^2$ ,  $n \approx n_l$ , we get the intrinsic birefringence

$$\Delta n_{\text{intr}} = C_V \frac{n_l}{\bar{n}} (n_1 - n_2) S_2 \quad (12)$$

and the form birefringence

$$\Delta n_{\text{form}} = - \frac{C_V}{2n_l \bar{n}^2} (\bar{n}^2 - n_l^2)^2 S_2 \quad (13)$$

In the case of  $S_2 = 1$  the latter expression is identical to the

formula derived for a regular assembly of thin parallel plates by Born and Wolf<sup>21</sup> assuming high dilution.

In order to apply these formulas to a sample of oriented purple membranes, we have to calculate the volume fraction of the particles. Since in purple membranes bacteriorhodopsin trimers form a two-dimensional hexagonal lattice, we get with the thickness of the particles  $t$ , Avogadro's constant  $N_A$ , the lattice constant  $a$ , the protein (bR) concentration  $C_{w/v}$  in (weight/volume), and the molecular weight of bR  $M$ :

$$C_V = t \frac{N_A}{3} \frac{\sqrt{3}}{2} a^2 \frac{C_{w/v}}{M} \quad (14)$$

Although our experiment supplies absorption, chromophore anisotropy, and the chromophore part of the linear birefringence as independent parameters, these quantities are connected via the Kramers–Kronig relations. As a useful control, to determine how accurate our experimental method works, we check whether the measured birefringence corresponds to the birefringence calculated from the anisotropic absorption. We start with the expression for the isotropic contribution to the refractive index due to absorption  $\delta n(\nu)$ , given in:<sup>20</sup>

$$\delta n(\nu) = \frac{\ln 10}{2\pi^2} c [C_{\text{bR}}] P \int_0^\infty \frac{\epsilon(\nu')}{\nu'^2 - \nu^2} d\nu' \quad (15)$$

where  $c$  is the velocity of light,  $[C_{\text{bR}}]$  the concentration in mol/L, and  $\epsilon(\nu)$  the decadic molar extinction coefficient.  $P$  indicates that the Cauchy principal value of the integral is to be taken. Considering a uniaxial sample and substituting  $\nu = c/\lambda$ ;  $d\nu = -c/\lambda^2 d\lambda$ ,  $A(\lambda) = \epsilon(\lambda)[C_{\text{bR}}]d$ , equation 15 yields:

$$\delta n_{||}(\lambda) = \frac{\ln 10}{2\pi^2 d} P \int_0^\infty \frac{A_{||}(\lambda')}{\left(1 - \frac{\lambda'}{\lambda}\right)\left(1 + \frac{\lambda'}{\lambda}\right)} d\lambda' \quad (16)$$

$$\delta n_{\perp}(\lambda) = \frac{\ln 10}{2\pi^2 d} P \int_0^\infty \frac{A_{\perp}(\lambda')}{\left(1 - \frac{\lambda'}{\lambda}\right)\left(1 + \frac{\lambda'}{\lambda}\right)} d\lambda' \quad (17)$$

With  $A_{||} - A_{\perp} = 3 A_0 r_A$ , the contribution to the birefringence is

$$\Delta n_A(\lambda) = \delta n_{||}(\lambda) - \delta n_{\perp}(\lambda) = \frac{3 \ln 10}{2\pi^2 d} P \int_0^\infty \frac{A_0(\lambda') r_A(\lambda')}{\left(1 - \frac{\lambda'}{\lambda}\right)\left(1 + \frac{\lambda'}{\lambda}\right)} d\lambda' \quad (18)$$

The preceding derivation assumed that the chromophore part is separable from the background, which requires a chromophore-free reference sample. But the formalism also allows the application to changes in the chromophore state, assuming only negligible changes in the scattering contribution:

$$E_0^I(\lambda) r_E^I(\lambda) - E_0^{II}(\lambda) r_E^{II}(\lambda) = A_0^I(\lambda) r_A^I(\lambda) - A_0^{II}(\lambda) r_A^{II}(\lambda) \quad (19)$$

and

$$\Delta n_E^I(\lambda) - \Delta n_E^{II}(\lambda) = \Delta n_A^I(\lambda) - \Delta n_A^{II}(\lambda) \quad (20)$$

where superscripts I and II denote two different chromophore

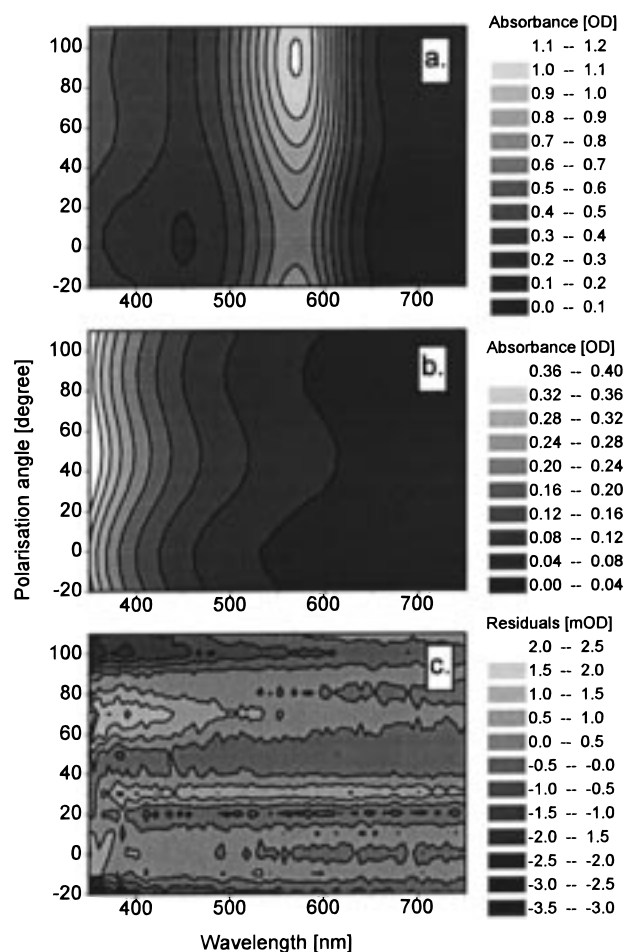


**Figure 3.** Contour plots of the polarized steady-state extinction  $E(\lambda, \theta)$  for a magnetically oriented sample,  $S_2 \approx +0.47$ , pH 7.0. (a) Purple membranes. (b) Chromophore free membranes. (c) Residuals of the fits of the data from the chromophore free membranes with eq 6.

states. From eq 18 we get for the difference of the contributions I and II to the birefringence:

$$\Delta n(\lambda) = \Delta n_A^I(\lambda) - \Delta n_A^{II}(\lambda) = \frac{3 \ln 10}{2\pi^2 d} P \int_0^\infty \frac{A_0^I(\lambda') r_A^I(\lambda') - A_0^{II}(\lambda') r_A^{II}(\lambda')}{\left(1 - \frac{\lambda'}{\lambda}\right) \left(1 + \frac{\lambda'}{\lambda}\right)} d\lambda' \quad (21)$$

## 4. Results

**4.1. Purple Membranes in the Light-Adapted State and Chromophore-Free Membranes.** The polarized extinctions  $E(\lambda, \theta)$ , averaged in wavelength over 5 nm intervals, of purple membranes in the light-adapted state and of chromophore free membranes are presented in the contour plots of Figure 3 (parts a and b, respectively). The purple membranes show a superposition of linear dichroism and linear birefringence effects, while in the chromophore-free membranes the linear birefringence is dominant. Both data blocks were fitted with eq 6 at each wavelength. The residuals of the fit of the data block related to the chromophore free membranes are presented in the contour plot of Figure 3c. In Figure 4 we plotted the data and the fit curves at two selected wavelengths,  $\lambda = 568$  nm (a, b) and  $\lambda = 633$  nm (c, d), for purple membranes (a, c) and chromophore-free membranes (b, d). Since the data and the fit curves are in excellent agreement, we conclude that the mathematical representation including linear dichroism and

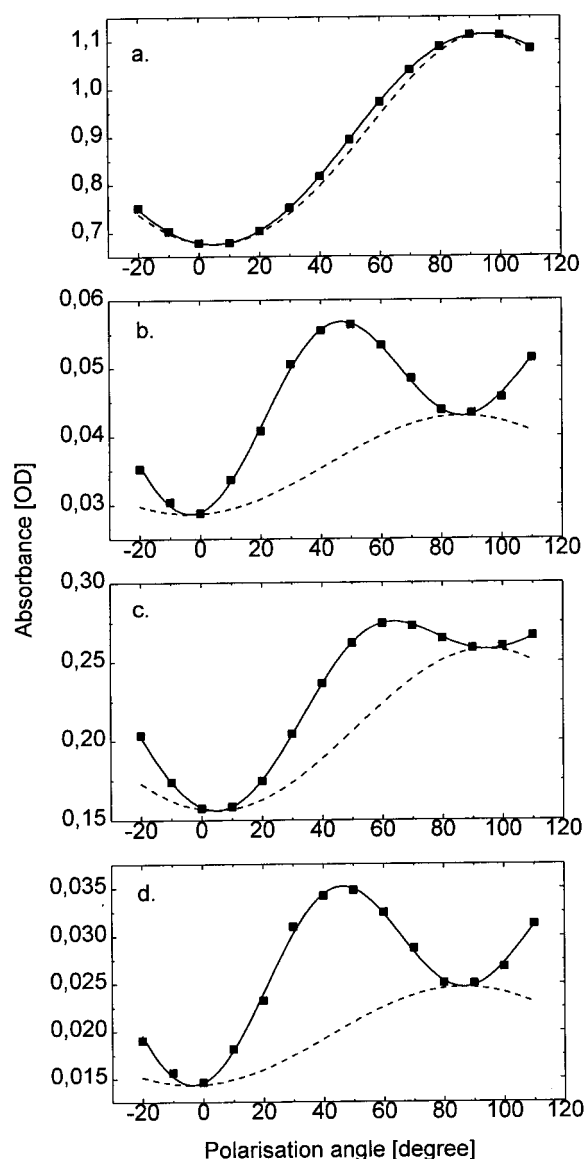


**Figure 4.** Sections of the polarized absorption data from Figure 3 at constant wavelengths. (a) purple membranes,  $\lambda = 568$  nm. (b) Chromophore-free membranes,  $\lambda = 568$  nm. (c) Purple membranes,  $\lambda = 633$  nm. (d) Chromophore-free membranes,  $\lambda = 633$  nm. The dashed lines indicate the dependence of the absorbance on the polarization angle in the absence of linear birefringence.

birefringence effects is correct. Optical activity (e.g., circular dichroism and circular birefringence) is negligible in our experiments. The dashed lines in Figure 4 indicate the dependence of the extinction (absorption and light scattering) on the polarization angle, which would be measured in the absence of linear birefringence. The higher the absorption, the lower is the relative contribution of the linear birefringence. But even at maximum absorption ( $\lambda = 568$  nm), the fit yields an accurate value for the phase difference ( $\Delta\phi_E = 27.6^\circ$ ).

The results of the fits  $E_0$ ,  $S_0$ ,  $r_E$ ,  $r_S$ ,  $\Delta n_E = (\Delta\phi_E/2\pi)(\lambda/d)$ , and  $\Delta n_S = (\Delta\phi_S/2\pi)(\lambda/d)$  are shown in Figure 5. From these parameters, we obtained the chromophore-related parameters  $A_0$ ,  $r_A$ , and  $\Delta n_A$  using eq 7. The chromophore absorption spectrum  $A_0$ , the chromophore anisotropy  $r_A$ , and the chromophore intrinsic birefringence  $\Delta n_A$  (anomalous dispersion) are plotted in Figures 5a, b, and d, respectively. From the absorption  $A_0 = 0.94$  at  $\lambda = 570$  nm (Figure 5a), we estimate that the concentration of our sample was  $C_{w/v} = 0.40$  mg/mL.

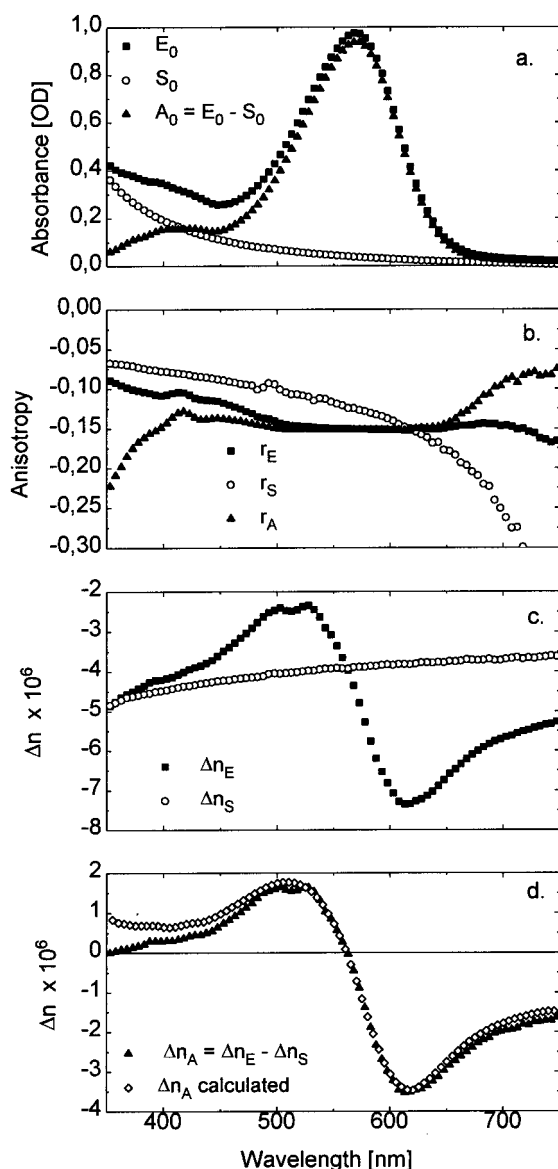


**Figure 5.** Results of the fitting procedure for purple membranes and chromophore free membranes. (a) Absorbance. (b) Anisotropy. (c) Linear birefringence. (d) Chromophore part of the linear birefringence, calculation with eq 18.

The absorption anisotropy  $r_A$  (Figure 5b) is about  $-0.15$  and nearly constant over the main visible absorption band  $500 \text{ nm} < \lambda < 650 \text{ nm}$ . Using the relation  $r_A = S_2 P_2(\cos \theta_0)^6$  and assuming  $\theta_0 = 70^\circ$ ,<sup>1,2</sup> we calculate the order parameter  $S_2 = 0.47$ .

The sign of the birefringence  $\Delta n_A$  was chosen by comparison with the theoretical expression for the chromophore contribution to the birefringence (eq 18). Due to the negative sign of  $r_A$ , the chromophore contribution to the birefringence  $\Delta n_A$  has negative sign in the wavelength region where  $\partial A(\lambda)/\partial \lambda$  is negative (e.g., for  $\lambda > 570 \text{ nm}$ ). From the sign of  $\Delta n_A$  it follows that  $\Delta n_E$  and  $\Delta n_S$  must have negative signs, since  $|\Delta n_E| > |\Delta n_S|$  for  $\lambda > 570 \text{ nm}$ . Numerical calculations of  $\Delta n_A$  from  $A_0$  and  $r_A$  have been carried out and compared with the experimentally determined curve ( $\Delta n_A = \Delta n_E - \Delta n_S$ ) (Figure 5d). Except for the deviations outside the main absorption band ( $\lambda < 500 \text{ nm}$  and  $\lambda > 650 \text{ nm}$ ), the experimental and the calculated curves agree very well.

**4.2. Light-Dark Adaptation.** The polarized extinctions  $E(\lambda, \theta)$ , averaged in wavelength over 5 nm intervals, of purple membranes in the light-adapted state and the dark-adapted (not

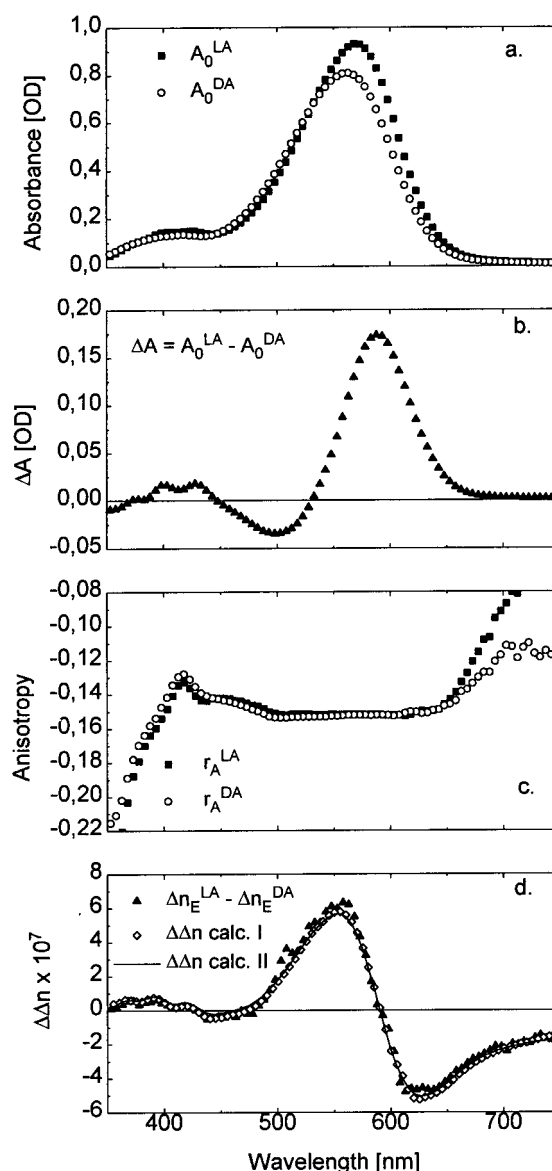


**Figure 6.** Results of the fitting procedure, light-dark adaptation, magnetically oriented sample,  $S_2 \approx +0.47$ , pH 7.0. (a) Absorbance. (b) Absorbance change. (c) Absorbance anisotropy. (d) Birefringence change, calculations using eq 21, I: with  $(A_0^{LA}(\lambda)r_A^{LA}(\lambda) - A_0^{DA}(\lambda)r_A^{DA}(\lambda))$ ; II: with  $\Delta A(\lambda)(-0.152)$ .

shown) were fitted with eq 6 at each wavelength. The data of purple membranes in the light-adapted state are the same as in the preceding section, and correction for light scattering was carried out in the same way. There is only a small shift in the spectra  $A_0^{LA}$  and  $A_0^{DA}$  (Figure 6a). The difference spectrum  $\Delta A(\lambda)$  (Figure 6b) is very similar to the absorption changes of dark adaptation measured by other authors,<sup>22,23</sup> including the small changes at 400 and 430 nm. The absorption anisotropies  $r_A^{LA}$  and  $r_A^{DA}$  (Figure 6c) are nearly identical. Obviously there is no measurable change in the orientation of the transition dipole moment during light-dark adaptation.

The measured birefringence changes  $\Delta \Delta n(\lambda)$  (Figure 6d) were compared with the calculations from the Kramers-Kronig relations, using eq 21. Instead of  $A_0^{LA}(\lambda)r_A^{LA}(\lambda) - A_0^{DA}(\lambda)r_A^{DA}(\lambda)$  in the nominator of the integrand the calculation has also been carried out with  $\Delta A(\lambda)$  and a constant anisotropy value of  $-0.152$ . Both calculations lead to close agreement with the measured birefringence changes. This is again a clear verification that the orientation of the transition dipole moment is

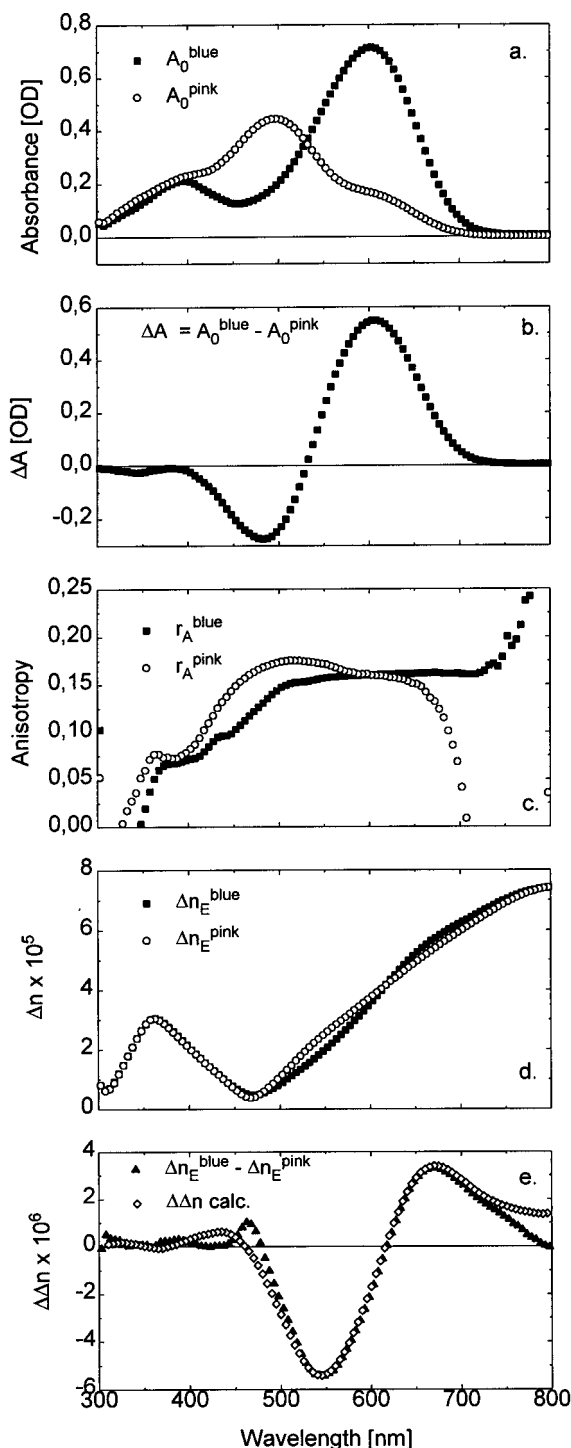


**Figure 7.** Results of the fitting procedure, blue–pink transition, sample oriented by swelling,  $S_2 \approx -0.49$ , pH 2.5. (a) Absorbance. (b) Absorbance change. (c) Absorbance anisotropy. (d) Linear birefringence. (e) Birefringence change, calculation using eq 21.

unaffected (in the limit of our experimental accuracy  $\Delta r = \pm 0.002$ ) by light–dark adaptation.

**4.3. Blue–Pink Transition.** The polarized extinctions  $E(\lambda, \theta)$ , averaged in wavelength over 5 nm intervals, of membranes in the blue state, the pink state, and the bleached retinal-free state were fitted with eq 6 at each wavelength. The results are shown in Figure 7, where the correction for light scattering has already been carried out. The absorption maximum shifts from about 605 nm in the blue state to 495 nm in the pink state (Figure 7a, and b). Since the blue to pink

transition is not complete, a shoulder around 610 nm occurs in the pink spectrum ( $A_0^{\text{pink}}(\lambda)$ ) corresponding to a fraction of molecules remaining in the blue state (20%). This fraction has been determined by down scaling of the blue spectrum so as to agree with the measured pink spectrum in the long-wavelength region ( $\lambda > 650$  nm). Even the blue spectrum ( $A_0^{\text{blue}}(\lambda)$ ) doesn't represent a single chromophore species. In Figure 7a the maxima at  $\lambda = 390$  nm in the blue spectrum ( $A_0^{\text{blue}}(\lambda)$ ) and the pink spectrum  $A_0^{\text{pink}}(\lambda)$  probably indicate a fraction of free retinal or contributions from higher absorption bands. The anisotropy of the blue state (Figure 7c) has a nearly constant value across the main absorption band ( $r_A^{\text{blue}} = 0.160 \pm 0.001$ ) and decreases with shorter wavelengths. This decrease might be an indication that the free retinal is disordered in the membranes. The higher absorption band may also contribute in this wavelength region. The anisotropy of the pink state is superimposed by the contributions of the blue state and free retinal, but at maximum absorption these contributions are relatively small and the maximum value  $r_A^{\text{pink}} = 0.175$  is close to the anisotropy of the pure pink state. Correcting for the 20% contribution of the blue state, we get  $r_A^{\text{pink}} = 0.179 \pm 0.001$  in the wavelength region  $505 \text{ nm} \leq \lambda \leq 555 \text{ nm}$ . Assuming  $\theta_{\text{blue}} = 70^\circ$ , the orientation of the transition dipole moment in the pink state is  $\theta_{\text{pink}} = 72.4^\circ$ , with respect to the membrane normal. In contrast to the magnetically oriented samples, in samples which were oriented by anisotropic swelling, significant contributions from stress birefringence occur and even dominate the other contributions. Therefore  $\Delta n_E^{\text{blue}}(\lambda)$  and  $\Delta n_E^{\text{pink}}(\lambda)$  show only small differences (Figure 7d). The measured birefringence changes  $\Delta \Delta n(\lambda)$  (Figure 7e) are in good agreement with the calculations from  $(A_0^{\text{blue}} r_A^{\text{blue}} - A_0^{\text{pink}} r_A^{\text{pink}})$  via the Kramers–Kronig relation, eq 21 though. The minor deviations at wavelengths  $< 500$  nm and  $> 700$  nm might arise from the fact, that the measured phase differences corresponding to  $\Delta n_E^{\text{blue}}(\lambda)$  and  $\Delta n_E^{\text{pink}}(\lambda)$  are close to  $0^\circ$  or  $180^\circ$  in these wavelength regions. Thus the measurements become insensitive, since the transmitted intensity scales with the cosine of the phase difference (see eq 5).

## 5. Discussion

**5.1. Significance of the Experimental Approach.** A very simple setup enables to measure linear dichroism and linear birefringence of oriented purple membrane samples over a spectral range from 300 nm to 800 nm. We only need a standard spectrophotometer and two Glan–Taylor polarizers, instead of an expensive experimental setup with Babinet–Soleil compensator and Pockels cell,<sup>15,24</sup> which is limited to birefringence measurements at discrete wavelengths. The measurement of the absorption as a function of the polarization angle assures determination of the anisotropy with high accuracy and reduces experimental artifacts by a second polarizer behind the sample. The phase sensitivity of our setup depends on the absolute value of the phase difference, since the transmitted intensity scales with the cosine of the phase difference according to eq 5. Consequently we have highest sensitivity at  $\Delta\phi = \pm 90^\circ, \pm 270^\circ$ , and lowest sensitivity at  $\Delta\phi = 0^\circ, \pm 180^\circ$ . The magnetically oriented purple membrane samples, which we normally use for flash photolysis ( $A(570 \text{ nm}) \approx 1 \text{ OD}$ ,  $S_2 \approx 0.5$ ), show phase differences from  $\Delta\phi_E = 16^\circ$  (at  $\lambda = 530 \text{ nm}$ ) to  $\Delta\phi_E = 43^\circ$  (at  $\lambda = 610 \text{ nm}$ ). Though we didn't have the optimal phase sensitivity, the comparison with calculations from absorption and anisotropy via the Kramers–Kronig transform indicates that our experimental method yields consistently the chromophore contribution to the birefringence of bR. The determination of

the anisotropy may be verified by the measured birefringence. This result means, however, that the experimental determination of the birefringence due to the chromophore doesn't supply additional information, if the complete visible spectrum is available. Under certain experimental conditions, where only discrete wavelengths are available, the measured birefringence change may provide useful information. Considering, for example, the isosbestic point of two chromophore states I and II, the absorbance change  $\Delta A = A_0^I - A_0^{II}$  is zero, while the birefringence change  $\Delta n = \Delta n_A^I - \Delta n_A^{II}$  reaches maximum value. The application of our experimental approach to time-resolved polarized spectroscopy (to be published), makes use of these birefringence measurements. The use of isotropically excited oriented samples is advantageous compared with the photoselection experiments of Tkachenko et al.<sup>25</sup>

**5.2. Contributions to the Refractive Index of Purple Membranes.** In order to compare our results with the measurements of other groups, we focus only on a single wavelength. At  $\lambda \approx 633$  nm our analysis yields  $\Delta n_E = -7.1 \times 10^{-6}$ ,  $\Delta n_S = -3.8 \times 10^{-6}$ ,  $\Delta n_A = -3.3 \times 10^{-6}$ , for a sample with an order parameter  $S_2 = 0.47$  and a concentration  $C_{w/v} = 0.40$  mg/mL. Since the birefringence  $\Delta n$  is proportional to the concentration  $C_{w/v}$  and the order parameter  $S_2$  according to eqs 9 and 14, the values are normalized to  $S_2 = 1$  (perfect orientation) and a protein concentration of  $C_{w/v} = 1$  mg/mL:  $\Delta n_E = -3.8 \times 10^{-5}$ ,  $\Delta n_S = -2.0 \times 10^{-5}$ ,  $\Delta n_A = -1.8 \times 10^{-5}$ . Normalized at the same protein concentration the birefringence obtained by Lewis et al.<sup>15</sup> extrapolated to infinite magnetic field strength is  $|\Delta n| = 3.2 \times 10^{-5}$ , which includes form birefringence and intrinsic birefringence. Considering the various sources of error and the scaling procedures the agreement is excellent. The slightly smaller value than our  $|\Delta n_E|$  might arise from a curvature of the membranes,<sup>26</sup> which lowers the effective order parameter  $S_2$ . Assuming a spherical curvature of the membranes with uniform curvature angle  $2\psi$ , the effective order parameter is reduced by a factor  $S_{\text{curv}} = 1/2(\cos^2 \psi + \cos \psi)$ . From eq 13 we get an estimate about the form birefringence of oriented purple membranes. With  $t = 50$  Å,  $a = 63$  Å,  $M = 26800$  g/mol and  $C_{w/v} = 1$  mg/mL we calculate the volume fraction of particles according to eq 14:  $C_V = 1.28 \times 10^{-3}$ . Thus the form birefringence is  $\Delta n_{\text{Form}} = -5.0 \times 10^{-5}$ , assuming  $n_l = 1.33$  and  $\bar{n} = 1.50$ . This value is of the right order of magnitude, but much larger than our measured birefringence of the bleached sample  $\Delta n_S = -2.0 \times 10^{-5}$ . A possible explanation might be that form birefringence as well as intrinsic birefringence contribute to  $\Delta n_S$  ( $\Delta n_S = \Delta n_{\text{Form}} + \Delta n_{\text{intr}}$ ). In consequence the intrinsic birefringence of the bleached sample would be  $\Delta n_{\text{intr}} = +3.0 \times 10^{-5}$ . From eq 12, assuming  $n_l/\bar{n} \approx 0.88$ , we calculate  $(n_1 - n_2) = -0.016$ , which is identical to the difference of the chromophore contributions ( $\delta n_1 - \delta n_2$ ). Considering eqs 16 and 17 in the case of perfect orientation ( $S_2 \equiv 1$ , i.e.,  $r_A = P_2(\cos \theta)$ ) and  $C_V = 1.0$ ,  $\delta n_{||} = \delta n_1$ , and  $\delta n_{\perp} = \delta n_2$ . The dependence on the chromophore angle is

$$\delta n_1 - \delta n_2 \sim 3P_2(\cos \theta_0), \quad \delta n_1 \sim 1 + 2P_2(\cos \theta_0) \\ \text{and} \quad \delta n_2 \sim 1 - P_2(\cos \theta_0) \quad (22)$$

From these relations it follows that

$$\delta n_1 = \frac{1 + 2P_2(\cos \theta_0)}{3P_2(\cos \theta_0)}(\delta n_1 - \delta n_2) \quad \text{and} \\ \delta n_2 = \frac{1 - P_2(\cos \theta_0)}{3P_2(\cos \theta_0)}(\delta n_1 - \delta n_2) \quad (23)$$

With  $\theta_0 = 70^\circ$  ( $P_2(\cos(70^\circ)) = -0.325$ ), we get  $\delta n_1 = +0.006$  and  $\delta n_2 = +0.022$ . The value  $\delta n_2$  may be interpreted as the contribution of the chromophore to the refractive index of purple membranes in the case of normal incidence (light beam perpendicular to membrane planes). In this respect the investigations of Zeisel and Hampp<sup>13</sup> provide comparable information. They measured light-induced refractive index and absorption changes in bR-films, using a modified Michelson interferometer. Continuous illumination of the films causes a photostationary equilibrium between the bR-groundstate and mainly the M-intermediate, which is spectroscopically characterized by a blue shifted spectrum ( $\lambda_{\text{max}} \approx 410$  nm,  $\epsilon(\lambda_{\text{max}}) \approx 45000$  M<sup>-1</sup> cm<sup>-1</sup>). The absorbance change and therefore the refractive index change is proportional to  $\eta$ , the fraction of molecules in the M-state. The calculation of the refractive index change from the measured retardation depends also on the volume fraction  $C_V$  of the purple membranes in the film. The connection between our  $\delta n_2$  and the quantity  $\Delta n$  measured by Zeisel and Hampp is hence

$$\Delta n = C_V \eta (\delta n_2 - \delta n_2^M) \quad (24)$$

We estimate numerically that  $\delta n_2^M$ , the contribution of M, is about 0.25 at  $\lambda = 633$  nm relative to the bR groundstate  $\delta n_2$ . In films of thickness  $25 \mu\text{m}$  and an absorption of 5 OD at  $\lambda = 570$  nm the volume fraction of the membranes  $C_V$  is about 0.8. In these films a modulation of the absorption of  $\Delta A = 0.55$  OD at  $\lambda = 633$  nm means that the fraction of excited molecules,  $\eta$ , we assume to be in the M-intermediate, is 0.5. Under these assumptions and with  $\delta n_2 = 0.022$  we get  $\Delta n = 0.0066$ , which is slightly smaller than the value of Zeisel and Hampp ( $\Delta n = 0.008$ ), but in the same order of magnitude. We note that there was an uncertainty in the scaling of their data.<sup>13</sup> Assuming a higher volume fraction of the membranes  $C_V$  or a higher fraction of excited molecules  $\eta$  or both, the results would agree better.

The determination of the refractive index of a bR film by Zhang et al.<sup>27</sup> should also reveal contributions of the chromophore to the refractive index. They used a modified critical-angle technique, where the probe beam was polarized in the plane of incidence, so one would expect that the measured  $\delta n$ -contribution is smaller than  $\delta n_2$  but larger than  $\delta n_1$ . But surprisingly in their measurements (accuracy  $\pm 0.002$ ) the dispersive behavior of the bR-film is similar to that of glass, and shows no anomalous effects due to the chromophore in the wavelength range from 410 to 675 nm.

**5.3. Reorientation of the Transition Dipole Moment.** The polarization measurements on thermally stable chromophore states provide information about changes in the orientation of the transition dipole moment. Since the dark-adapted state is a mixture of all-trans, 15-anti (<sup>1</sup>/<sub>3</sub>) and 13-cis,15-syn (<sup>2</sup>/<sub>3</sub>) retinal isomers,<sup>7</sup> the anisotropy of the dark-adapted state differs from the anisotropy of the light-adapted state if the isomerization is associated with a reorientation of the transition dipole moment in which the angle with the membrane normal changes. Our measurements didn't show anisotropy changes, so we conclude that the orientation of the transition dipole moment is unchanged ( $\Delta\theta = \pm 0.2^\circ$ ) by the isomerization. This is in close agreement with the measurements on bR-crystals by Schertler et al.,<sup>11</sup> who estimated only a small change of about  $0.8^\circ$ .

According to Balashov et al.,<sup>28</sup> the dark-adapted state of blue membranes (pH 2.5) is also a mixture of all-trans and 13-cis-15-syn retinal isomers, but with a higher fraction (nearly 60%) of all-trans-bR than in the purple state at pH 7.0. Since there is no reorientation of the transition dipole moment in light—



dark adaptation of purple membranes, we assume that this is also the case in light–dark adaptation of blue membranes. Therefore the mixture of isomers in the dark adapted state of blue membranes has no influence on the reorientation of the retinal in the blue to pink transition. From the measured anisotropies  $r_{\text{blue}} = 0.160$  and  $r_{\text{pink}} = 0.179$  and assuming  $\theta_{\text{blue}} = 70^\circ$ , we calculate  $\theta_{\text{pink}} = 72.4^\circ$ . This change of  $2.4^\circ$  depends only weakly on the unknown value of  $\theta_{\text{blue}}$  as long as  $\theta_{\text{blue}}$  is not too far away from  $70^\circ$  ( $68^\circ$  and  $72^\circ$  lead to  $\Delta\theta$ -values of  $2.0^\circ$  and  $3.0^\circ$ , respectively.) The change of  $2.4^\circ$  is a surprisingly small value, considering, that the blue to pink transition is accompanied by isomerization around the 9–10 double bond in the middle of the polyene chain. We point out that with our method we are not able to detect an angular change in the plane parallel to the membrane. One way to understand the small angular changes of the transition dipole moment in the light–dark and blue–pink transitions comes from experiments on the chromophore orientation in the M-intermediate (13-cis). Neutron diffraction<sup>29</sup> and  $^2\text{H-NMR}$ <sup>30</sup> experiments indicate that the polyene chain tilts out of the plane of the membrane in the transition from all-trans (bR) to 13-cis (M) by  $10^\circ$  and  $4^\circ$ , respectively. The observed change in the transition dipole moment angle on the other hand was only  $2 - 3^\circ$ .<sup>4</sup> This smaller difference could be explained by assuming that the transition dipole moment vector connects the  $\beta$ -ionone ring with the Schiff base nitrogen and does not change much in direction when one part of the polyene chain tilts up and the other part tilts down in the isomerization. It seems that the retinylidene chromophore is strongly fixed in the binding pocket by the linkage to the lysine 216 side chain on the Schiff-base end and by steric limitations of the  $\beta$ -ionone ring at the other end.

## Conclusions

With oriented purple membrane samples between parallel polarizers, we have measured the extinction as a function of the angle between polarizer- and orientation-axis. In this way accurate data could be obtained on the wavelength-dependent absorption anisotropy and linear birefringence due to the retinylidene chromophore of bacteriorhodopsin. Calculations using the Kramers–Kronig transform confirmed that these data are internally consistent. From the birefringence data we estimate, that the contribution of the chromophore to the refractive index of purple membranes in the case of normal incidence is approximately 0.022 at 633 nm. The purple membranes were oriented in a 14 T magnetic field and immobilized in a gel. Better orientation was achieved by a novel method in which an isotropic purple membrane gel is dehydrated and subsequently allowed to rehydrate and to swell in only one dimension. These methods were used to monitor changes in the angle between the electronic transition dipole moment and the orientation axis which may occur when the chromophore

isomerizes. No change in this angle was observed during light–dark adaptation when the chromophore configuration changes from all-trans,15-anti to 13-cis,15-syn. In the light induced blue to pink transition, in which the chromophore configuration changes from all-trans to 9-cis, a change of only  $2.4^\circ$  was observed. These very small orientation changes of the electronic transition dipole moment suggest that the end points of the polyene chain remain fixed during these isomerizations.

**Acknowledgment.** This research was supported by the Deutsche Forschungsgemeinschaft, Grant He1382/7-2.

## References and Notes

- (1) Heyn, M. P.; Cherry, R. J.; Müller, U. *J. Mol. Biol.* **1977**, *117*, 607.
- (2) Lin, S. W.; Mathies, R. A. *Biophys. J.* **1989**, *56*, 653.
- (3) Dér, A.; Hargittai, P.; Simon, J. J. *Biochem. Biophys. Methods* **1985**, *54*, 295.
- (4) Otto, H.; Heyn, M. P. *FEBS Lett.* **1991**, *293*, 111.
- (5) Heyn, M. P.; Otto, H. *Photochem. Photobiol.* **1992**, *56*, 1105.
- (6) Otto, H.; Zscherp, C.; Borucki, B.; Heyn, M. P. *J. Phys. Chem.* **1995**, *99*, 3847.
- (7) Scherrer, P.; Mathew, M. K.; Sperling, W.; Stoeckenius, W. *Biochemistry* **1989**, *28*, 829.
- (8) Fischer, U.; Oesterheld, D. *Biophys. J.* **1979**, *28*, 211.
- (9) Maeda, A.; Iwasa, T.; Yoshizawa, T. *Biochemistry* **1980**, *19*, 3825.
- (10) Liu, S. Y.; Ebrey, T. G. *Photochem. Photobiol.* **1987**, *46*, 263.
- (11) Schertler, G. F. X.; Lozier, R.; Michel, H.; Oesterheld, D. *EMBO J.* **1991**, *10*, 2353.
- (12) Peterlin, A.; Stuart, H. A. *Z. Phys.* **1939**, *112*, 129.
- (13) Zeisel, D.; Hampp, N. *J. Phys. Chem.* **1992**, *96*, 7788.
- (14) Dér, A.; Tóth-Boconádi, R.; Keszthelyi, L.; Kramer, H.; Stoeckenius, W. *FEBS Lett.* **1995**, *377*, 419.
- (15) Lewis, B. A.; Rosenblatt, C.; Griffin, R. G.; Courtemanche, J.; Herzfeld J. *Biophys. J.* **1985**, *47*, 143.
- (16) Abdourakhmanov, I. A.; Ganago, A. O.; Erokhin, Y. E.; Solov'ev, A. A.; Chugunov, V. A. *Biochim. Biophys. Acta* **1979**, *546*, 183.
- (17) Ganago, A. O.; Fok, M. V.; Abdourakhmanov, I. A.; Solov'ev, A. A.; Erokhin, Y. E. *Mol. Biol. (Moscow)* **1980**, *14*, 381.
- (18) Govindjee, R.; Balashov, S. P.; Ebrey, T. G. *Biophys. J.* **1990**, *58*, 597.
- (19) Fowles, G. R. *Introduction to Modern Optics*, 2nd ed.; Holt, Rinehart and Winston: New York, 1975; Chapter 2.
- (20) Klier, D. S.; Lewis, J. W.; Randall, C. E. *Polarized Light in Optics and Spectroscopy*, 1st ed.; Academic Press: San Diego, 1990; Chapter 4.
- (21) Born, M.; Wolf, E. *Principles of Optics*, 1st ed.; Pergamon Press: New York, 1959; Chapter 14.
- (22) Balashov, S. P.; Imasheva, E. S.; Govindjee, R.; Sheves, M.; Ebrey, T. G. *Biophys. J.* **1996**, *70*, 473.
- (23) Kouyama, T.; Bogomolni, R. A.; Stoeckenius, W. *Biophys. J.* **1985**, *48*, 201.
- (24) Maret, G.; Weill, G. *Biopolymers* **1983**, *22*, 2727.
- (25) Tkachenko, N. V.; Savransky, V. V.; Sharonov, A. Y. *Eur. Biophys. J.* **1989**, *17*, 131.
- (26) Czégé, J.; Reinisch, L. *Biophys. J.* **1990**, *58*, 721.
- (27) Zhang, C.; Song, Q. W.; Gross, R. B.; Birge, R. R. *Optics Letters* **1994**, *19*, 1409.
- (28) Balashov, S. P.; Imasheva, E. S.; Govindjee, R.; Sheves, M.; Ebrey, T. G. *Biophys. J.* **1996**, *71*, 1973.
- (29) Hauss, T.; Büldt, G.; Heyn, M. P.; Dencher, N. A. *Proc. Natl. Acad. Sci. U.S.A.* **1994**, *91*, 11854.
- (30) Ulrich, A. S.; Wallat, I.; Heyn, M. P.; Watts, A. *Nature Struct. Biol.* **1995**, *2*, 190.